J Mol Hist (2017) 48:99–111
DOI 10.1007/s10735-016-9709-9

ORIGINAL PAPER

Muscarinic acetylcholine receptor-mediated tight junction opening is involved in epiphora in late phase of submandibular gland transplantation

Ning-Yan Yang[1,2] · Chong Ding[3] · Jing Li[1] · Yan Zhang[4] · Ruo-Lan Xiang[4] · Li-Ling Wu[4] · Guang-Yan Yu[1] · Xin Cong[4]

Received: 1 December 2016 / Accepted: 27 December 2016 / Published online: 11 January 2017

Abstract Submandibular gland (SMG) autotransplantation is an effective therapy for treating severe dry eye syndrome. However, epiphora occurs in more than 40% of patients 6 months after operation. We previously found that muscarinic acetylcholine receptor (mAChR) plays a crucial role in regulating SMG secretion partially through the modulation on tight junction (TJ)-based paracellular pathway. Therefore, the present study aimed to investigate the possible involvement of mAChR and TJ in a rabbit long-term model of SMG transplantation. We found that SMG secretion was significantly increased on postoperative days 90 and 180, which imitated epiphora observed in the patients with SMG transplantation. Although the mRNA expression and fluorescence intensity of M1 and M3 mAChR subtypes were reversed to control levels on postoperative days 30, 90, and 180, the content of β-arrestin2, but not β-arrestin1, was gradually decreased after transplantation, which suggests that mAChR may be hypersensitive in late phase of SMG transplantation. The width of acinar TJs was enlarged and fluorescence intensity of F-actin in peri-apicolateral membranes were remarkably increased on postoperative days 90 and 180. Topical treatment with atropine gel significantly reduced SMG secretion, TJ width, as well as F-actin intensity in peri-apicolateral membranes on postoperative days 180. Moreover, in a perfused rabbit SMG, carbachol increased salivary secretion, enlarged TJ width, and induced F-actin rearrangement, whereas these responses were inhibited by atropine pretreatment. Taken together, our findings suggest that the hypersensitive mAChR may contribute to epiphora in late phase of SMG transplantation through modulating TJ-based paracellular permeability.

Keywords Muscarinic acetylcholine receptor · Transplantation · Tight junction · Submandibular gland · Secretion

✉ Xin Cong
congxin634@126.com

[1] Department of Oral and Maxillofacial Surgery, Peking University School and Hospital of Stomatology, National Engineering Laboratory for Digital and Material Technology of Stomatology, and Beijing Key Laboratory of Digital Stomatology, Beijing 100081, People's Republic of China

[2] Department of Pediatric Dentistry, Beijing Stomatological Hospital and School of Stomatology, Capital Medical University, Beijing 100050, People's Republic of China

[3] Central Laboratory, Peking University School and Hospital of Stomatology, Beijing 100081, People's Republic of China

[4] Department of Physiology and Pathophysiology, Peking University School of Basic Medical Sciences, and Key Laboratory of Molecular Cardiovascular Sciences, Ministry of Education, Beijing Key Laboratory of Cardiovascular Receptors Research, Beijing 100191, People's Republic of China

Introduction

Dry eye syndrome, also known as keratoconjunctivitis sicca, is a common ophthalmological disease characterized by reduced or absent tears and has serious complications, such as progressive destruction of corneal surface and even loss of vision (Sieg et al. 2000; Yu et al. 2004). Although the usage of pharmaceutical tear substitution and the occlusion of lacrimal drainage pathway can relieve the discomfort for the patients with wild and moderate dry eye syndrome, these therapies show unsatisfactory effects on severely affected patients. Microvascular transplantation of autologous submandibular gland (SMG) into the temporal fossa with insertion of the Wharton's duct into the upper conjunctival fornix was first reported in 1986

(Murube-del-Castillo 1986). The transplanted SMG provides a continuous and endogenous source of ocular lubrication to replace insufficient tears (Murube-del-Castillo 1986; Yu et al. 2004). Since then, this technique has been identified to be a lasting and effective strategy for patients with severe dry eye syndrome to improve clinical manifestations and reduce corneal damage (Geerling et al. 1998; Murube-del-Castillo 1986; Sieg et al. 2000; Yu et al. 2004). However, it is notable that during the operation, SMG artery and vein are anastomosed with the facial vessels, while the nerve is cut without anastomosis, which may cause an alteration in the secretory pattern after transplantation. Clinical investigation has shown that more than 40% of patients suffer from epiphora 6 months after surgery, and this discomfort is more serious during physical activity or in a hot environment (Geerling et al. 2008; Yu et al. 2004). The part of transplanted SMG has to be resected to reduce the secretion for patients with severe epiphora. Therefore, it is essential to explore the epiphora mechanism and find an effective therapeutic method to prevent the occurrence of epiphora and to avoid more operations.

Fluid and electrolyte secretion in salivary glands is primarily evoked by the activation of muscarinic acetylcholine receptor (mAChR) and α-adrenoceptor (Baum 1993; Melvin et al. 2005). Previous studies showed that down-regulated mAChR signaling pathway is associated with the early hyposecretion of transplanted SMG in rabbit, while elevated mRNA and protein expressions of M1 and M3 subtype receptors is observed in transplanted glands from epiphora patients (Ding et al. 2014; Shi et al. 2010). These results suggest that alterations of mAChR might play a dominant role in salivation of transplanted SMGs. Recently, the importance of tight junction (TJ)-mediated paracellular pathway in modulating salivary secretion has gained much attention. Studies on rabbit and rat isolated perfused SMGs reported that the majority of water is transported through paracellular pathway (Murakami et al. 2001; Steward et al. 1990). Functional measurement showed that the paracellular permeability of SMG-C6 cells is increased in response to activation of mAChR, while the disruption in TJ barrier is seen in minor salivary gland from Sjögren's syndrome patients (Cong et al. 2015, 2013; Ewert et al. 2010). Interferon-γ upregulates claudin-7 expression and increases epithelial barrier function in human SMG duct epithelium (Abe et al. 2016). These studies indicate that the change or disturbance in salivary TJs may influence the permeability of paracellular pathway as well as production of saliva. However, it is still unknown whether paracellular pathway contributes to epiphora in late phase of SMG transplantation.

Therefore, by establishing a rabbit long-term model of SMG autotransplantation, we aimed to investigate the dynamic changes of mAChR and paracellular pathway, and further explored the mechanism involved in the modulation of paracellular pathway in transplanted SMGs.

Materials and methods

Animals

Healthy male New Zealand white rabbits weighing 2.3–2.5 kg were used. All experimental procedures were approved by the Ethics Committee of Animal Research, Peking University Health Science Center, and the investigation conformed to the guide for the care and use of laboratory animals (NIH Publication No. 85-23, revised 1996). All animal research is reported in accordance with the ARRIVE guidelines (Kilkenny et al. 2010).

Reagents and antibodies

Carbachol, atropine, and FITC-labeled phalloidin were purchased from Sigma–Aldrich (MO, USA). Atropine sulfate eye gel was purchased from Shenyang Xing Qi Pharmaceutical Co. LTD (Shenyang, Liaoning, China). Antibodies to M1 and M3 receptors, β-arrestin1, β-arrestin2, β-actin, horseradish peroxidase- and FITC-conjugated secondary antibodies were purchased from Santa Cruz Biotechnology (Carlsbad, CA, USA). Other chemicals and reagents were of analytical grade.

SMG transplantation model

Microvascular autologous transplantation of SMG was performed as described previously with a minor modification (Shi et al. 2010; Yang et al. 2013). Briefly, under anesthesia with sodium pentobarbital (20 mg/kg body weight), the left SMG along with its Wharton's duct and related blood vessels were transplanted to the right temporal region. The free gland was revascularized by anastomosis of the lingual artery branch to the distal part of the external carotid artery and the facial vein branch to the temporal vein. Meanwhile, the Wharton's duct was transferred under the temporal skin with a reconstructed duct that opened in the lower conjunctival fold. Saliva secretion was measured and the glands were removed at 7, 30, 90, and 180 days after operation under anesthesia for further investigation (n = 6 per group). The sham-operated SMGs without transplantation were used as controls (n = 6). To explore the role of mAChR in the occurrence of epiphora, atropine sulfate eye gel, a non-selective mAChR antagonist, was smeared on the temporal skin over the transplanted gland (2 × 2 cm^2) 180 days after operation (n = 3). The secretion was measured 15 min after the topical treatment of atropine gel.

Measurement of secretion

Saliva was collected from a cannula inserted into the Wharton's duct of both control and transplanted gland 24 h prior to the measurement. Saliva flow was measured by Schirmer's test using a moistened length of filter paper (35 mm × 5 mm) recorded for 5 min (Lopez-Jornet et al. 2006). All measurements were performed between 9:00 and 10:00 am in resting conscious conditions.

Perfusion of isolated SMG

Under anesthesia, rabbit SMG was isolated and perfused with Krabs-Ringer Hepes (KRH) solution (120 mmol/L NaCl, 5.4 mmol/L KCl, 1 mmol/L $CaCl_2$, 1 mmol/L $MgCl_2$, 0.96 mmol/L NaH_2PO_4, 11.1 mmol/L glucose, 20 mmol/L HEPES, pH 7.4) aerated with 95% O_2 at a rate of 3 mL/min through a polyethylene cannula inserted into the external carotid artery. After equilibration for 30 min, the gland was infused with carbachol (0.1 μmol/L) for 10 min with or without pretreatment of atropine (0.1 μmol/L). Saliva secretion was measured as the relative area of moisture on the filter paper and glands were collected for further investigation.

Real-time polymerase chain reaction (PCR)

Total RNA was isolated from homogenized gland tissue with use of Trizol reagent (Invitrogen, Carlsbad, CA, USA) according to manufacturer's instructions. Four micro grams of RNA pretreated with DNase I was used to amplify cDNA by use of M-MLV reverse transcriptase and primed with oligo-dT using RevertAid™ First Strand cDNA Synthesis Kit (Thermo Fisher Scientific, Waltham, MA, USA). A total reaction mixture volume of 5 μL 2 × qPCR Mix, 1 μL cDNA, 1 μL primers, 0.2 μL 50 × passive reference dye, and 2.8 μL ddH_2O were used for PCR amplification by using DyNAmo Color Flash SYBR Green qPCR Kit in Piko-Real PCR Systems (Thermo Fisher Scientific). The cDNA was amplified at 94 °C for 10 min, followed by 40 cycles at 94 °C for 30 s, 56 °C for 40 s, and 72 °C for 40 s. Dissociation curves were generated for each sample to confirm the specificity of the amplification. The sense and antisense primers for rabbit M1 (GenBank ID: XM_002720993.1), M3 (XM_002717330.1), M5 (XM_002712153.1) receptors and β-actin were 5′-TTCTGGCAATATCTGGTAGG-3′ and 5′-ACAGTGACAGGGAGGTAG-3′; 5′-GCACCA TTCTCAACTCTACC-3′ and 5′-CCATCATCTACGCTC TTCTG-3′; 5′-CCGAGTCTTCCAAGCGGTCTA-3′ and 5′-GGAGGGAGCAGGGCATGATT-3′; 5′-CACGAGACC ACCTTCAAC-3′ and 5′-CCGATTCACACCGAGTAC-3′.

Immunofluorescence

SMGs were fixed in 4% paraformaldehyde and frozen sections (7 μm thick) were prepared. Microwave antigen retrieval was performed by using 0.01 mol/L citric acid buffer, and then the sections were incubated with antibodies against M1 and M3 receptors (dilution: 1:100) at 4 °C overnight and FITC-labeled secondary antibodies at 37 °C for 2 h. For the staining of filamentous actin (F-actin), sections were directly incubated with FITC-phalloidin at 37 °C for 2 h. Fluorescence images were captured with a confocal microscope (Leica TCS SP5, Wetzlar, Germany) and the average fluorescence intensity from ten randomly chosen acini from each section was measured by ImageJ Software (National Institutes of Health, Bethesda, MD, USA).

Transmission electron microcopy

SMG tissues were fixed in 2% paraformaldehyde-1.25% glutaraldehyde, and then sliced into ultrathin sections. The sections were stained with uranyl acetate and lead citrate, and examined with a transmission electron microscope (HITACHI H-7000, Tokyo, Japan). The average TJ distance between neighboring acinar cells (shown as TJ width) from ten randomly chosen regions in each section was measured by ImageJ Software as described previously (Nighot and Blikslager 2010).

Western blot analysis

SMGs were homogenized in lysis buffer (50 mmol/L Tris–HCl, 150 mmol/L NaCl, 1 mmol/L ethylenediamine tetraacetic acid, 1 mmol/L phenylmethylsulfonyl fluoride, 1% Triton X-100, 0.1% SDS, and 0.1% sodium deoxycholate, pH 7.2) by use of a polytron homogenizer as described previously (Yang et al. 2013). The lysates were centrifuged and the supernatants were collected. Crude protein extracts (40 μg) were separated on 9% SDS-PAGE and transferred to polyvinylidene difuoride membranes. The membranes were blocked with 5% non-fat milk, probed with antibodies for M1 (dilution: 1:500), M3 receptors (dilution: 1:500), β-arrestin1 (dilution: 1:200), and β-arrestin2 (dilution: 1:200) at 4 °C overnight, and then incubated with horseradish peroxidase-conjugated secondary antibodies at room temperature for 2 h. Immunoreactive bands were visualized by enhanced chemiluminescence reagent (Thermo Scientific Pierce, Rockford, IL, USA). The density of bands was scanned and quantified by ImageJ Software. Membranes were striped and reprobed with antibody for β-actin to assure equal loading.

Statistical analysis

Data are shown as mean ± S.E.M. Differences among groups were analyzed by one-way analysis of variance (ANOVA) followed by Bonferroni's test. Value of $P < 0.05$ was considered significant.

Results

The secretion of transplanted SMG is increased in the late phase

The basal secretory flow of SMG in control group was 1.29 ± 0.22 mm/min. After transplantation, the secretion was significantly decreased to a barely detected level on postoperative days 7 ($P < 0.01$, Fig. 1), while it was recovered to control level on postoperative days 30, and further significantly increased on postoperative days 90 and 180. These results suggested that the secretory pattern in rabbit SMG transplantation model could imitate the hyposecretion and epiphora phenomenon seen in patients during early and late phases after SMG transplantation.

The expression of mAChR is upregulated in the late phase of transplanted SMG

mAChR plays a crucial role in the production of saliva (Melvin et al. 2005; Shi et al. 2010). To explore whether mAChR was changed in transplanted glands, we detected the mRNA levels of two mAChR subtypes expressed in rabbit SMGs. Real-time PCR analysis revealed that the mRNA expression of M1 and M3 receptors were substantially decreased on postoperative days 7, while they were recovered to control levels from 30 to 180 days after operation (Fig. 2a, b). By contrast, the mRNA expression of M5 receptor, which was particularly expressed in endothelial cells, remained unchanged among different time points (Fig. 2c).

The distribution of mAChR determines its normal function. In control SMGs, M1 receptor was mainly localized at the apical membranes of acinar cells and cytoplasm, while M3 receptor was diffusely distributed in the cytoplasm. However, the fluorescence intensities of both M1 and M3 receptors were significantly diminished on postoperative days 7, whereas they were recovered to normal levels on postoperative days 30, 90, and 180 (Fig. 2d). Quantification analysis further confirmed these changes (Fig. 2e, f).

In addition to the expression level, the sensitivity of mAChR also affects the receptor activity. We have observed that intracellular Ca^{2+} is significantly increased in isolated human epiphora SMGs compared to controls, which suggest that hypersensitive mAChR may be involved in epiphora (Ding et al. 2014). Here, we detected the protein levels of β-arrestin1 and β-arrestin2, which can bind to agonist-activated phosphorylated G protein-coupled receptors and then terminate the receptor activation (Krupnick and Benovic 1998; Moore et al. 2007). Our results showed that the protein expression of β-arrestin1 did not change among different time points in the transplanted SMGs, while β-arrestin2 was significantly decreased on postoperative days 90 and 180 (Fig. 3).

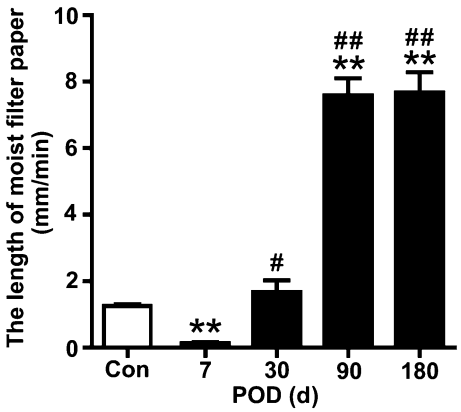

Fig. 1 Salivary secretion in rabbit transplanted submandibular glands. The salivary flow rate (mm/min) was measured by Schirmer's test on postoperative days 7, 30, 90, and 180. *Con* control gland, *POD* post-operative day. Data are mean ± S.E.M. of six independent experiments. $^{**}P < 0.01$ compared with controls. $^{\#}P < 0.05$ and $^{\#\#}P < 0.01$ compared with the secretion on postoperative days 7

TJ width is increased in the late phase of transplanted SMG

TJ acts as a gatekeeper in regulating the movement of water, solutes, and small particles through paracellular pathway (Kuo et al. 2014; Tsukita et al. 2001). The width of TJs between adjacent cells is a common used index of TJ function (Zhang et al. 2013). In control glands, TJ appeared as a narrow and continuous seal at the apical portion between neighboring acini by a transmission electron microscope, while TJ ultrastructure became obscure and its width was significantly reduced on postoperative days 7 (Fig. 4). However, the TJ ultrastructure became vivid and the width of TJs recovered to control level on postoperative days 30, and even markedly increased on postoperative days 90 and 180 (260.84 and 299.45% of control, respectively), suggesting that the acinar TJ is significantly opened in the late phase of transplanted SMGs.

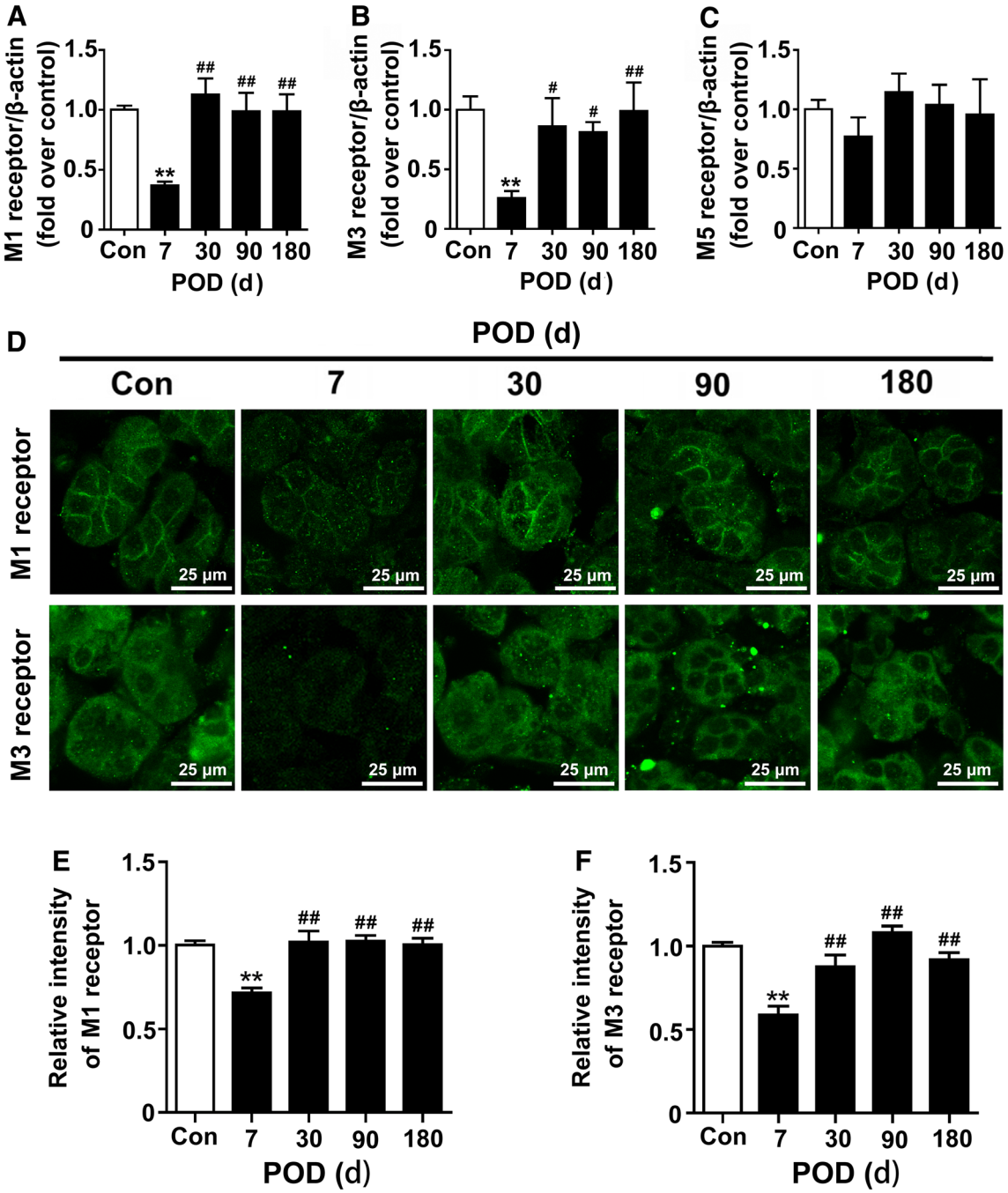

Fig. 2 Expression and distribution of mAChR in rabbit transplanted submandibular glands. (**a**–**c**) The mRNA expression of M1 (**a**), M3 (**b**), and M5 (**c**) receptors in the transplanted glands were detected on postoperative days 7, 30, 90, and 180 by real-time PCR. (**d**) The distribution of M1 and M3 receptors were observed with a confocol microscope by immunofluorescence staining. Bars 25 μm. (**e**–**f**) Quantitative analysis of fluorescence intensity of M1 (**e**) and M3 (**f**) receptors was performed in nine randomly selected acini in each section from six independent experiments. *Con* control gland, *POD* post-operative day. Data are mean ± S.E.M. of six independent experiments. $^{**}P < 0.01$ compared with controls. $^{\#}P < 0.05$ and $^{\#\#}P < 0.01$ compared with the fluorescence intensity on postoperative days 7

F-actin is accumulated to peri-apicolateral region in the late phase of transplanted SMG

F-actin directly binds to TJ proteins, and herein, the change in F-actin morphology would affect the structure and function of TJ (Bruewer et al. 2004). We found that F-actin was predominantly expressed at peri-apicolateral membranes in control glands. The fluorescence intensity of F-actin was significantly reduced at peri-apicolateral membranes on postoperative days 7, while recovered to

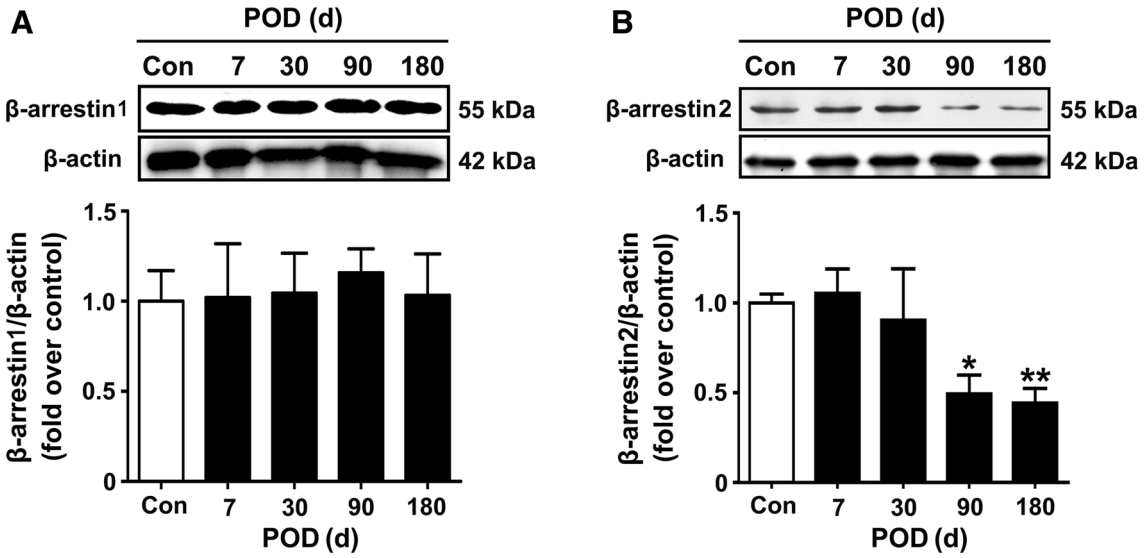

Fig. 3 Expression of β-arrestin1 and β-arrestin2 in rabbit transplanted submandibular glands. The protein levels of β-arrestin1 (**a**) and β-arrestin2 (**b**) were detected in the transplanted glands on postoperative days 7, 30, 90, and 180 by western blot, and semi-quantitative analysis of band intensity was shown below. *Con* control gland, *POD* post-operative day. Data are mean ± S.E.M. of six independent experiments. $^{*}P<0.05$ and $^{**}P<0.01$ compared with controls

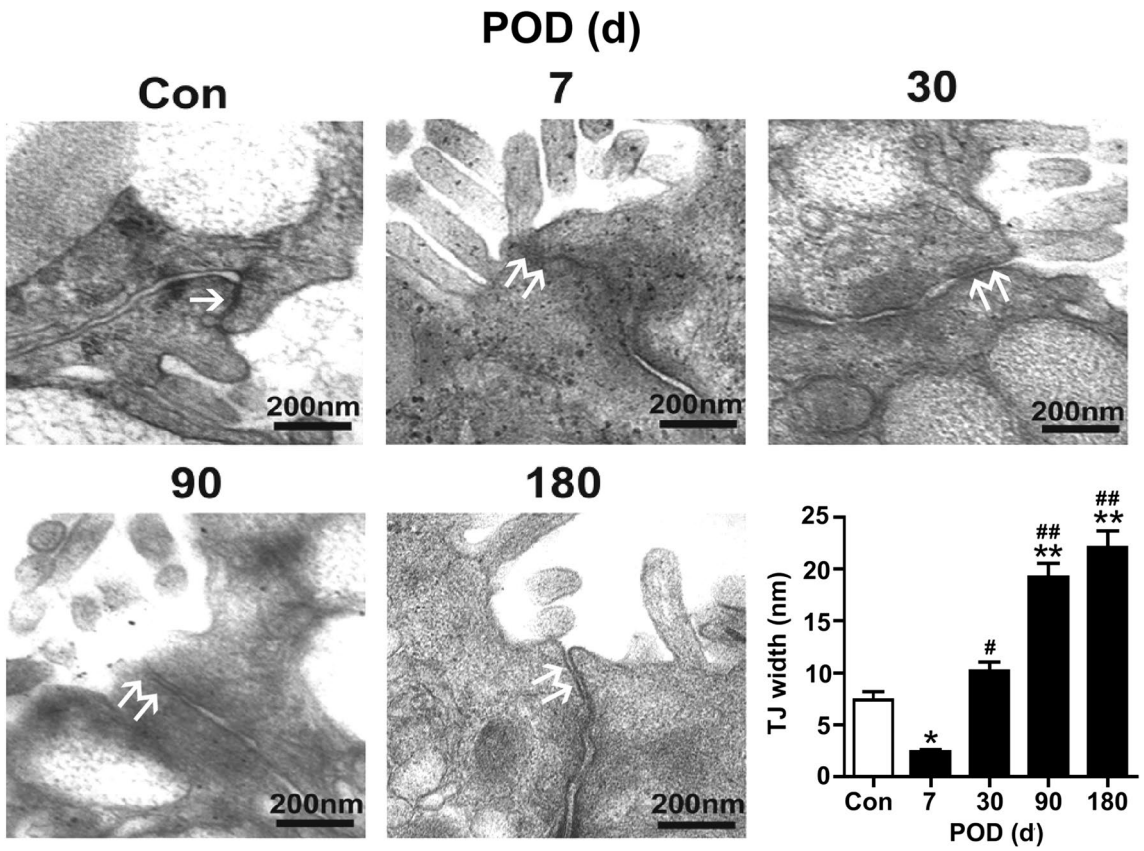

Fig. 4 Ultrastructure of acinar tight junctions (TJs) in rabbit transplanted submandibular glands. Representative images of TJ ultrastructure in control and transplanted glands, and the width of apical TJs was measured from five sections of ten random fields in each section. *Con* control gland, *POD* post-operative day. $^{*}P<0.05$ and $^{**}P<0.01$ compared with controls. $^{\#}P<0.05$ and $^{\#\#}P<0.01$ compared with the TJ width on postoperative days 7

control level on postoperative days 30 and even more significant on postoperative days 90 and 180 compared with control glands (Fig. 5a). Semi-quantitative analysis on the apicolateral F-actin intensity further confirmed these phenomena (Fig. 5b). Meanwhile, the total intensity of F-actin in acini was significantly decreased on postoperative days 7, whereas restored to control levels on postoperative days 30, 90, and 180 (Fig. 5c), which suggested that the dynamic redistribution of F-actin might contribute to TJ alteration observed in transplanted SMGs.

Atropine decreases secretion and TJ width in the late phase of transplanted SMG

Previous studies show that activation of mAChR can regulate salivary TJs and thereby alter the permeability of paracellular pathway (Cong et al. 2015). Accordingly, we explored whether the hypersecretion observed in the long-term transplanted SMGs was associated with the effect of mAChR on TJs. Topical treatment with atropine gel, a non-selective antagonist of mAChR, significantly reduced the secretory flow by 70% in the transplanted glands on postoperative days 180 (Fig. 6a), suggesting that activation of mAChR plays a dominant role in the occurrence of hypersecretion in the long-term phase. Moreover, altered TJ ultrastructure as well as distended TJ width in the transplanted gland on postoperative days 180 were inhibited by treatment with atropine gel (Fig. 6b, c). In addition, the aggregation of F-actin at peri-apicolateral membranes on postoperative days 180 was partially attenuated by atropine treatment (Fig. 6d–f). These results indicate that inhibition of mAChR blocks the hypersecretion and the opening of TJs in the late phase of transplanted SMGs.

Activation of mAChR increases TJ width and alters F-actin distribution in perfused rabbit SMG

To identify whether activation of mAChR directly modulates TJs in SMGs, we performed a perfusion assay by using freshly isolated rabbit SMGs. Infusion with carbachol

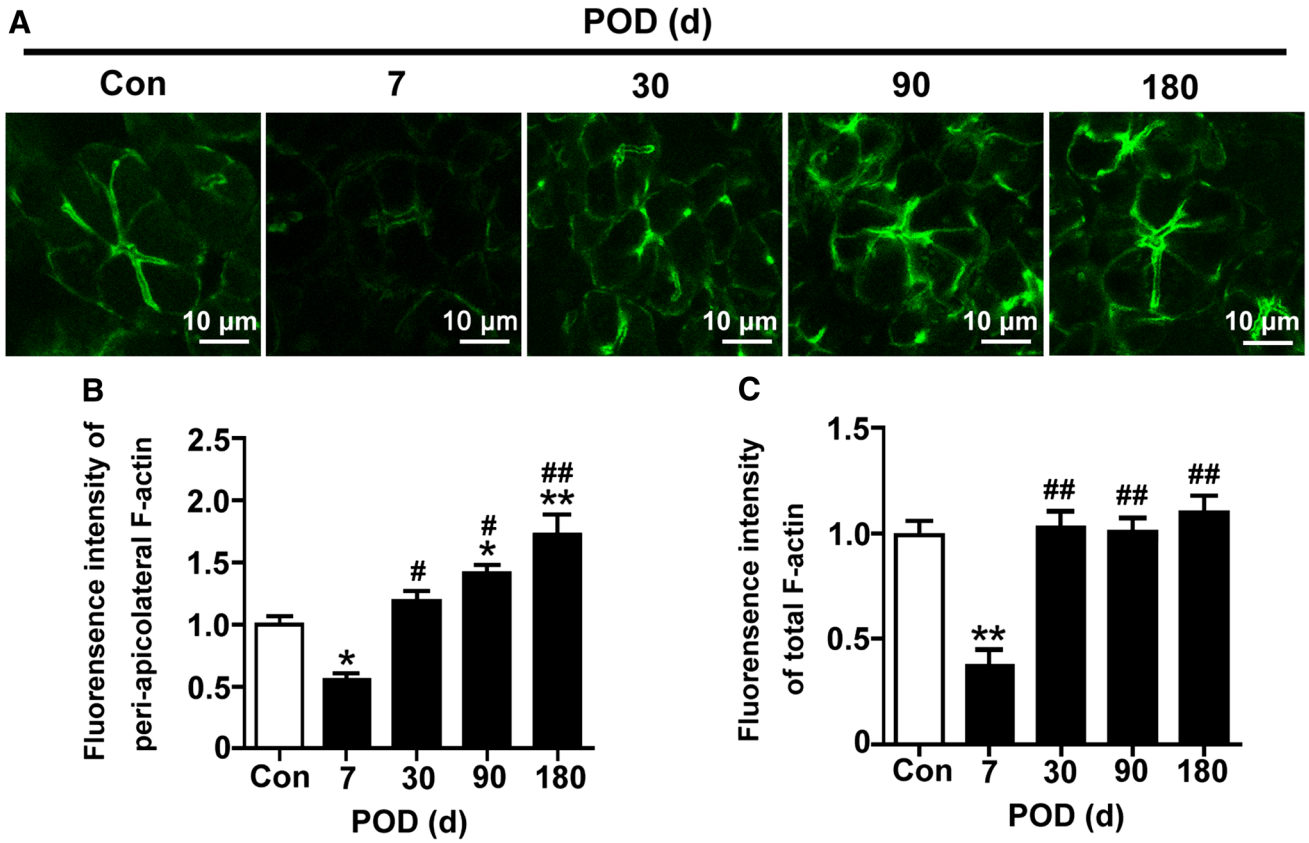

Fig. 5 Distribution of filamentous actin (F-actin) in rabbit transplanted submandibular glands. (**a**) Representative images of F-actin in control and transplanted glands by confocal miscroscopy. Bars 10 μm. (**b**–**c**) Quantitative analysis of fluorescence intensity was performed in nine randomly selected acini in each section from 6 independent experiments, and shown by the intensity of F-actin in peri-apical membranes (**b**) and the intensity of total F-actin in each acinus (**c**). *Con* control gland, *POD* post-operative day. Data are mean ± S.E.M. of six independent experiments. $^{*}P < 0.05$ and $^{**}P < 0.01$ compared with controls. $^{\#}P < 0.05$ and $^{\#\#}P < 0.01$ compared with the fluorescence intensity on postoperative days 7

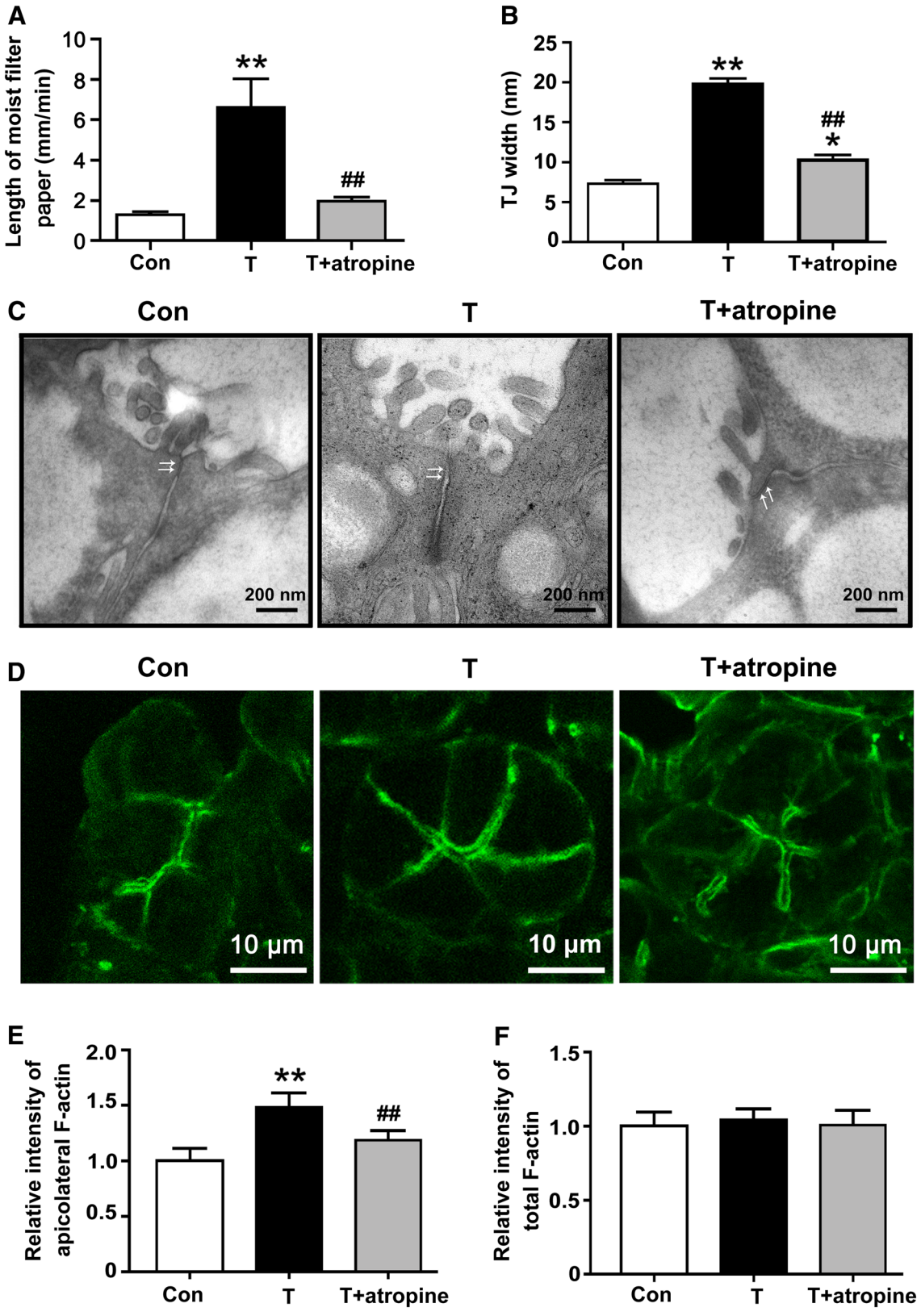
A
Length of moist filter paper (mm/min)
10
8
6
4
2
0
**
##
Con
T
T+atropine
B
TJ width (nm)
25
20
15
10
5
0
**
##
*
Con
T
T+atropine
C
Con
T
T+atropine
200 nm
200 nm
200 nm
D
Con
T
T+atropine
10 μm
10 μm
10 μm
E
Relative intensity of apicolateral F-actin
2.0
1.5
1.0
0.5
0
**
##
Con
T
T+atropine
F
Relative intensity of total F-actin
1.5
1.0
0.5
0
Con
T
T+atropine

◂**Fig. 6** Effect of atropine on the secretion, tight junction (TJ) ultrastructure, and F-actin distribution in rabbit transplanted submandibular glands on postoperative days 180. (**a**) Atropine gel was smeared on the skin of transplanted glands, and salivary flow rate was detected by Schirmer's test. (**b**–**c**) After treatment with atropine, the ultrastructure of acinar TJs was observed with a transmission electron microscope, and the width of neighboring TJs was measured using ImageJ software. (**d**–**f**) Representative images of F-actin in control, transplanted, and transplanted glands with atropine treatment (**d**), and the intensity of F-actin in peri-apical membranes (**e**) and the intensity of total F-actin in each acinus (**f**) were quantified using ImageJ software. *Con* control gland, *T* transplanted, *T+atropine* transplanted glands with atropine treatment, *POD* post-operative day. Data are mean ± S.E.M. of 6 independent experiments. $^{**}P < 0.01$ compared with controls. $^{\#\#}P < 0.01$ compared with transplanted groups

(0.1 μmol/L, 10 min) from the external carotid artery significantly increased the secretion of isolated glands. Pretreatment with atropine (0.1 μmol/L) for 10 min abolished carbachol-induced secretion (Fig. 7a). Electron microscope images showed that the distance between neighboring TJs was enlarged in carbachol-treated SMGs, whereas this effect was inhibited by atropine pretreatment (Fig. 7b, c). Moreover, the carbachol-induced accumulation of F-actin towards apical membranes was attenuated by atropine pretreatment, which suggests that the redistribution of F-actin is the direct effect caused by activation of mAChR (Fig. 7d–f).

Discussion

In the present study, by establishing a hypersecretion model of long-term rabbit SMG transplantation, we demonstrated that the sensitivity of mAChR was significantly increased in the late stage of transplanted SMGs. Moreover, the neighboring acinar TJ was opened and the distribution of F-actin was reorganized accompanying with the hypersecretion in late phase of SMG transplantation. Pretreatment with atropine could reduce TJ opening, abolish F-actin reorganization, and inhibit increased secretion in long-term transplanted SMGs. In addition, perfusion with carbachol in isolated rabbit SMGs directly increased the secretion and changed the structure of TJ and F-actin, whereas pretreatment with atropine abolished these responses. These findings suggest the hypersensitive mAChR might contribute to epiphora in long-term transplanted SMGs through modulating TJ-based paracellular permeability.

Nowadays, SMG autotransplantation is considered to be an effective therapy to treat severe dry eye syndrome (Yu et al. 2004). However, since the SMG nerves are cut off, the salivary secretion alters after transplantation (Geerling et al. 1998; Su et al. 2015, 2013). During 1 week to 3 months after operation, patients usually experience "latent period", which means the secretion gradually declines. Afterwards, epiphora may occur in more than 40% of patients after 6 months, and severe epiphora can lead to social embarrassment and blurred vision. We previously established a short-term rabbit SMG transplantation model, in which the secretion was substantially decreased and barely detectable on postoperative days 4–7, a pattern similar to that seen in "latent period" of patients with SMG transplantation (Cong et al. 2012; Shi et al. 2010; Yu et al. 2004; Zhang et al. 2010). The mechanism of hyposecretion in early phase of SMG transplantation is associated with decreased expression of M1 and M3 receptors a substantial reduction in neurotransmitter release, and downregulated intracellular signaling molecule. The topical application of carbachol is shown to increase the secretion and improve parenchymal atrophy in early phase of transplanted glands (Shi et al. 2010). However, to date, the secretory mechanism of the long-term transplanted SMGs is not fully understood. In the present study, we established a long-term rabbit SMG transplantation model, and found that the secretion was recovered to control levels on postoperative days 30, while further increased on postoperative days 90 and 180, which suggest that the transplanted SMG enters into a hypersecretory state at days 90 and 180 after operation.

In salivary glands, fluid secretion is mainly mediated by activation of mAChR. Previous studies showed that the changes in mAChR expression and function is involved in the radiation therapy-induced xerostomia, Sjögren's syndrome, as well as the xerostomia caused by a large number of drugs including antidepressants, antihistamines, and antispasmodics (Scully 2003; Sumida et al. 2013; Wiseman and Faulds 1995). The low dose pilocarpine-stimulated salivary flow rate is dramatically reduced by ~90% in M3 receptor-knockout mice and ~50% in M1 receptor-knockout mice, while almost completely abolished in M1 and M3 receptor double-knockout mice (Gautam et al. 2004). These results indicate that both M1 and M3 receptors play important roles in regulating salivary secretion. Here, by establishing a rabbit long-term SMG transplantation model, we found that the mRNA expression of M1 and M3 receptors were significantly decreased on postoperative days 7, which was in accordance with the previous study (Shi et al. 2010), whereas they were recovered to control levels on postoperative days 30, 90 and 180. Immunofluorescence images also showed that the intensities of M1 and M3 receptors in acinar cells were reversed to control levels in the long-term transplanted SMGs. However, the alteration of mAChR expression was not consistent with the secretory pattern in the late stage, and this finding was different from the previous study in human epiphora SMGs which shows an upregulated expression in M1 and M3 receptors (Ding et al. 2014). We consider the differences might be due to the different species. Besides, considering that mAChR is found to be hypersensitive in SMGs from epiphora patients (Ding et al. 2014), we detected mAChR sensitivity in

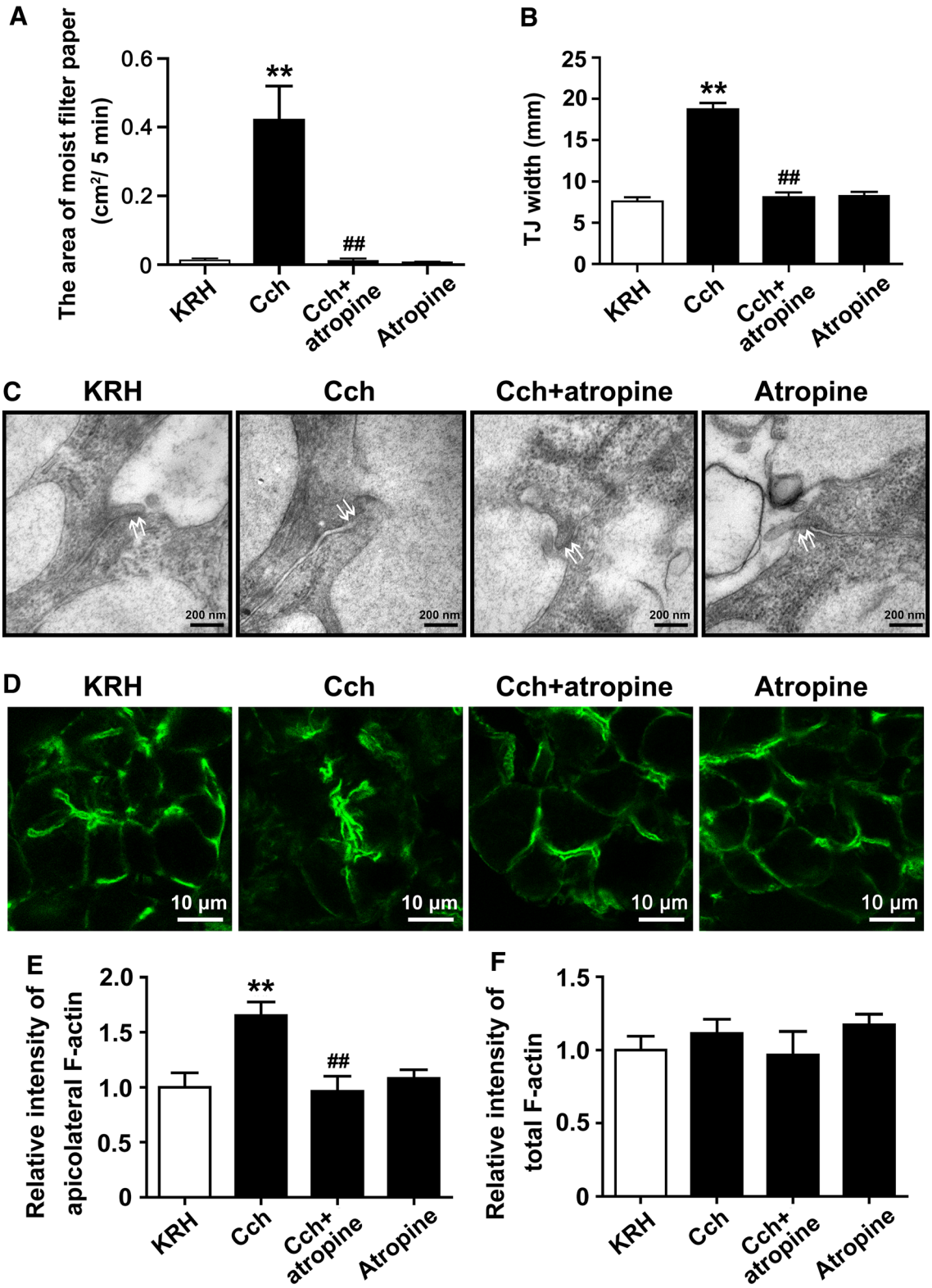

rabbit transplanted hypersecretory glands. β-arrestin1/2 can bind to the agonist-activated phosphorylated G protein-coupled receptors, trigger the receptor internalization by clathrin-coated pits, and then terminate G protein activation (Krupnick and Benovic 1998; Luo et al. 2008; Moore et al. 2007). It has been reported that knockdown of β-arrestin1 or β-arrestin2 significantly increases the carbachol-induced calcium mobilization (Luo et al. 2008),

◂**Fig. 7** Effect of carbachol and atropine pretreatment on the secretion, tight junction (TJ) ultrastructure, and F-actin distribution in rabbit isolated submandibular glands. (**a**) The isolated glands were perfused with carbachol with or without atropine pretreatment, and salivary secretion was shown as the relative area of moisture on the filter paper. (**b–c**) Representative images of TJ ultrastructure in the isolated submandibular glands treated with carbachol with or without atropine pre-perfusion, and TJ width was measured using ImageJ software. (**d–f**) Representative images of F-actin in KRH, carbachol, carbachol and atropine, and atropine alone glands (**d**). The intensity of F-actin in peri-apical membranes (**e**) and the intensity of total F-actin in each acinus (**f**) were quantified using ImageJ software. *KRH* KRH solution, *Cch* carbachol, *Cch + atropine* carbachol and atropine. Data are mean ± S.E.M. of six independent experiments. $^{**}P < 0.01$ compared with KRH. $^{\#\#}P < 0.01$ compared with carbachol-treated groups

which suggest that β-arrestin1/2 may partially represent the activity of mAChR. In the present study, we found a gradually reduced expression of β-arrestin2, but not β-arrestin1, in the transplanted hypersecretory glands, implying that although the expression level of M1 and M3 receptors did not show significant increases, but their sensitivities were significantly increased in parallel with the increased secretion in late stage of transplanted SMGs.

TJ-based paracellular pathway is an important route for water, ion, and solute transport across diverse epithelia and endothelia (Gonzalez-Mariscal et al. 2003). To date, increasing advances in studying TJ have been made regarding to its important role in the regulation of paracellular permeability in renal, intestine, corneal, epidermal epithelia, as well as in the barrier function, such as blood–brain barrier and blood-testis barrier (Chung et al. 2001; Fleegal et al. 2005; Furuse et al. 2002; Iwamoto et al. 2014; Muto et al. 2010; Tamura et al. 2011). In SMG epithelium, TJ constitutes a crucial route for the formation of saliva (Zhang et al. 2013). Activation of mAChR selectively regulates TJ expression and distribution, and thereby increases the paracellular permeability in SMG cells (Cong et al. 2015). Aberrant expression and distribution of TJ proteins and disruption in TJ barrier are seen in salivary glands from Sjögren's syndrome patients and animal models (Ewert et al. 2010; Zhang et al. 2016). Moreover, we previously found that TJ expression and structure are impaired and paracellular permeability is decreased in rabbit hypofunctional transplanted SMG during early stage (Cong et al. 2012). However, whether TJ-based paracellular pathway is involved in epiphora is still unknown. In this study, we found that the width of acinar apical TJs was recovered to control levels on postoperative days 30, while further increased on postoperative days 90 and 180. We also observed the distribution of F-actin, which directly connects with TJ proteins and plays an important role in regulating TJ structure. Images showed that the intensity of F-actin at peri-apicolateral membranes was decreased on postoperative days 7, while recovered on postoperative days 30. The staining of F-actin turned to be more accumulated to apicolateral membranes of acini on postoperative days 90 and 180. These results suggest that TJ opening and F-actin rearrangement might contribute to the hypersecretion in the long-term transplanted SMGs.

To further explore whether mAChR participated in the hypersecretion in transplanted glands through TJ-based paracellular pathway, topical treatment with atropine gel was performed on transplanted glands on postoperative days 180. Results showed that smearing with atropine could significantly reduce the secretory flow, inhibit the increase in TJ width, and recover the rearrangement of F-actin. These results suggest that although the content of M1 and M3 receptors in rabbit long-term transplanted SMGs is similar to control level, mAChR still plays a key role in the occurrence of epiphora probably due to its hypersensitivity, and hence, the inhibition of mAChR show effective effects in the prevention of epiphora through regulating the opening of TJs.

To avoid the interference of nerve and humor system in vivo, we also performed the isolated SMG perfusion assay. Perfusion with carbachol rapidly and directly increased the salivary secretion and the TJ width, caused the rearrangement of F-actin, whereas pretreatment with atropine inhibited these alterations, a phenomenon similar to the above in vivo experiment. These results demonstrate that activation of mAChR directly regulates TJ opening and F-actin distribution, and hence increases the salivation in rabbit SMG. Moreover, inhibition of mAChR could be a promising treatment for the excessive secretion occurred in SMG transplantation.

In summary, our studies established a rabbit long-term SMG transplantation model and found that the sensitivities of M1 and M3 receptors were increased in epiphora glands. Activation of mAChR induced the opening of TJ-based paracellular pathway, increased secretion in the long-term transplanted SMGs, while these effects could be inhibited by use of atropine. Our findings enrich the understanding of the secretory mechanism and identify mAChR as a potential therapeutic target to treat epiphora in the long-term SMG transplantation.

Acknowledgements This study was supported by the National Natural Science Foundation of China 81470756 (NYY), 81300893 (XC), and 81400526 (GYY), and Beijing Natural Science Foundation 7154204 (NYY).

Author contributions NYY performed the major experiments and wrote the manuscript. CD, JL, YZ and RLX were responsible for the isolation and perfusion of rabbit submandibular gland. LLW and GYY participated in data interpretation and manuscript improvement. XC designed the study, analyzed the data, and wrote the manuscript. All authors read and approved the final manuscript.

Compliance with ethical standards

Conflict of interest The authors declare that they have no competing interests.

References

Abe A, Takano K, Kojima T, Nomura K, Kakuki T, Kaneko Y, Yamamoto M, Takahashi H, Himi T (2016) Interferon-gamma increased epithelial barrier function via upregulating claudin-7 expression in human submandibular gland duct epithelium. J Mol Histol 47:353–363. doi:10.1007/s10735-016-9667-2

Baum BJ (1993) Principles of saliva secretion. Ann N. Y. Acad Sci 694:17–23

Bruewer M, Hopkins AM, Hobert ME, Nusrat A, Madara JL (2004) RhoA, Rac1, and Cdc42 exert distinct effects on epithelial barrier via selective structural and biochemical modulation of junctional proteins and F-actin. Am J Physiol Cell Physiol 287:C327–C335. doi:10.1152/ajpcell.00087.2004

Chung NP, Mruk D, Mo MY, Lee WM, Cheng CY (2001) A 22-amino acid synthetic peptide corresponding to the second extracellular loop of rat occludin perturbs the blood-testis barrier and disrupts spermatogenesis reversibly in vivo. Biol Reprod 65:1340–1351

Cong X, Zhang Y, Shi L et al (2012) Activation of transient receptor potential vanilloid subtype 1 increases expression and permeability of tight junction in normal and hyposecretory submandibular gland. Lab Invest 92:753–768. doi:10.1038/labinvest.2012.12

Cong X, Zhang Y, Yang NY et al (2013) Occludin is required for TRPV1-modulated paracellular permeability in the submandibular gland. J Cell Sci 126:1109–1121. doi:10.1242/jcs.111781

Cong X, Zhang Y, Li J et al (2015) Claudin-4 is required for modulation of paracellular permeability by muscarinic acetylcholine receptor in epithelial cells. J Cell Sci 128:2271–2286. doi:10.1242/jcs.165878

Ding C, Cong X, Zhang Y, Yang NY, Li SL, Wu LL, Yu GY (2014) Hypersensitive mAChRs are involved in the epiphora of transplanted glands. J Dent Res 93:306–312. doi:10.1177/0022034513519107

Ewert P, Aguilera S, Alliende C et al (2010) Disruption of tight junction structure in salivary glands from Sjogren's syndrome patients is linked to proinflammatory cytokine exposure. Arthritis Rheum 62:1280–1289. doi:10.1002/art.27362

Fleegal MA, Hom S, Borg LK, Davis TP (2005) Activation of PKC modulates blood-brain barrier endothelial cell permeability changes induced by hypoxia and posthypoxic reoxygenation. Am J Physiol Heart Circ Physiol 289:H2012–H2019. doi:10.1152/ajpheart.00495.2005

Furuse M, Hata M, Furuse K et al (2002) Claudin-based tight junctions are crucial for the mammalian epidermal barrier: a lesson from claudin-1-deficient mice. J Cell Biol 156:1099–1111. doi:10.1083/jcb.200110122

Gautam D, Heard TS, Cui Y, Miller G, Bloodworth L, Wess J (2004) Cholinergic stimulation of salivary secretion studied with M1 and M3 muscarinic receptor single- and double-knockout mice. Mol Pharmacol 66:260–267. doi:10.1124/mol.66.2.260

Geerling G, Sieg P, Bastian GO, Laqua H (1998) Transplantation of the autologous submandibular gland for most severe cases of keratoconjunctivitis sicca. Ophthalmology 105:327–335

Geerling G, Garrett JR, Paterson KL et al (2008) Innervation and secretory function of transplanted human submandibular salivary glands. Transplantation 85:135–140. doi:10.1097/01.tp.0000296060.39823.a4

Gonzalez-Mariscal L, Betanzos A, Nava P, Jaramillo BE (2003) Tight junction proteins. Prog Biophys Mol Biol 81:1–44

Iwamoto N, Higashi T, Furuse M (2014) Localization of angulin-1/LSR and tricellulin at tricellular contacts of brain and retinal endothelial cells in vivo. Cell Struct Funct 39:1–8

Kilkenny C, Browne WJ, Cuthill IC, Emerson M, Altman DG (2010) Improving bioscience research reporting: The ARRIVE guidelines for reporting animal research. J Pharmacol Pharmacother 1:94–99. doi:10.4103/0976-500X.72351

Krupnick JG, Benovic JL (1998) The role of receptor kinases and arrestins in G protein-coupled receptor regulation. Annu Rev Pharmacol Toxicol 38:289–319. doi:10.1146/annurev.pharmtox.38.1.289

Kuo TM, Luo SY, Chiang SL et al (2014) Arecoline induces TNF-alpha production and Zonula Occludens-1 redistribution in mouse Sertoli TM4 cells. J Biomed Sci 21:93. doi:10.1186/s12929-014-0093-z

Lopez-Jornet P, Camacho-Alonso F, Bermejo-Fenoll A (2006) A simple test for salivary gland hypofunction using oral Schirmer's test. J Oral Pathol Med 35:244–248. doi:10.1111/j.1600-0714.2006.00411.x

Luo J, Busillo JM, Benovic JL (2008) M3 muscarinic acetylcholine receptor-mediated signaling is regulated by distinct mechanisms. Mol Pharmacol 74:338–347. doi:10.1124/mol.107.044750

Melvin JE, Yule D, Shuttleworth T, Begenisich T (2005) Regulation of fluid and electrolyte secretion in salivary gland acinar cells. Annu Rev Physiol 67:445–469. doi:10.1146/annurev.physiol.67.041703.084745

Moore CA, Milano SK, Benovic JL (2007) Regulation of receptor trafficking by GRKs and arrestins. Annu Rev Physiol 69:451–482. doi:10.1146/annurev.physiol.69.022405.154712

Murakami M, Shachar-Hill B, Steward MC, Hill AE (2001) The paracellular component of water flow in the rat submandibular salivary gland. J Physiol 537:899–906

Murube-del-Castillo J (1986) Transplantation of salivary gland to the lacrimal basin. Scand J Rheumatol Suppl 61:264–267

Muto S, Hata M, Taniguchi J et al (2010) Claudin-2-deficient mice are defective in the leaky and cation-selective paracellular permeability properties of renal proximal tubules. Proc Natl Acad Sci USA 107:8011–8016. doi:10.1073/pnas.0912901107

Nighot PK, Blikslager AT (2010) ClC-2 regulates mucosal barrier function associated with structural changes to the villus and epithelial tight junction. Am J Physiol Gastrointest Liver Physiol 299:G449–G456. doi:10.1152/ajpgi.00520.2009

Scully C (2003) Drug effects on salivary glands: dry mouth. Oral Dis 9:165–176

Shi L, Cong X, Zhang Y et al (2010) Carbachol improves secretion in the early phase after rabbit submandibular gland transplantation. Oral Dis 16:351–359. doi:10.1111/j.1601-0825.2009.01633.x

Sieg P, Geerling G, Kosmehl H, Lauer I, Warnecke K, von Domarus H (2000) Microvascular submandibular gland transfer for severe cases of keratoconjunctivitis sicca. Plast Reconstr Surg 106:554–560. (**discussion 561–552**)

Steward MC, Seo Y, Rawlings JM, Case RM (1990) Water permeability of acinar cell membranes in the isolated perfused rabbit mandibular salivary gland. J Physiol 431:571–583

Su JZ, Liu XJ, Zhang L, Yu GY (2013) Schirmer test in transplanted submandibular gland: influencing factors and a modified measurement method. Cornea 32:419–422. doi:10.1097/ICO.0b013e31825aba2c

Su JZ, Cai ZG, Yu GY (2015) Microvascular autologous submandibular gland transplantation in severe cases of keratoconjunctivitis sicca. Maxillofac Plast Reconstr Surg 37:5. doi:10.1186/s40902-015-0006-4

Sumida T, Tsuboi H, Iizuka M, Asashima H, Matsumoto I (2013) Anti-M3 muscarinic acetylcholine receptor antibodies in

patients with Sjogren's syndrome. Mod Rheumatol 23:841–845. doi:10.1007/s10165-012-0788-5

Tamura A, Hayashi H, Imasato M et al (2011) Loss of claudin-15, but not claudin-2, causes Na+ deficiency and glucose malabsorption in mouse small intestine. Gastroenterology 140:913–923. doi:10.1053/j.gastro.2010.08.006

Tsukita S, Furuse M, Itoh M (2001) Multifunctional strands in tight junctions. Nat Rev Mol Cell Biol 2:285–293. doi:10.1038/35067088

Wiseman LR, Faulds D (1995) Oral pilocarpine: a review of its pharmacological properties and clinical potential in xerostomia. Drugs 49:143–155

Yang NY, Shi L, Zhang Y et al (2013) Ischemic preconditioning reduces transplanted submandibular gland injury. J Surg Res 179:e265–e273. doi:10.1016/j.jss.2012.02.066

Yu GY, Zhu ZH, Mao C et al (2004) Microvascular autologous submandibular gland transfer in severe cases of keratoconjunctivitis sicca. Int J Oral Maxillofac Surg 33:235–239. doi:10.1006/ijom.2002.0438

Zhang Y, Cong X, Shi L et al (2010) Activation of transient receptor potential vanilloid subtype 1 increases secretion of the hypofunctional, transplanted submandibular gland. Am J Physiol Gastrointest Liver Physiol 299:G54–G62. doi:10.1152/ajpgi.00528.2009

Zhang GH, Wu LL, Yu GY (2013) Tight junctions and paracellular fluid and ion transport in salivary glands. Chin J Dent Res 16:13–46

Zhang LW, Cong X, Zhang Y et al (2016) Interleukin-17 impairs salivary tight junction integrity in Sjogren's syndrome. J Dent Res 95:784–792. doi:10.1177/0022034516634647